Magnetic Domain Formation in Itinerant Metamagnets

B. Binz,[1,2,3,*] H. B. Braun,[1,4] T. M. Rice,[1] and M. Sigrist[1]

[1]*Theoretische Physik, ETH Zurich, CH-8093 Zurich, Switzerland*
[2]*Department of Physics, University of Fribourg, Chemin du Musée 3, CH-1700 Fribourg, Switzerland*
[3]*Department of Physics, University of California, 366 Le Conte #7300, Berkeley, California 94720-7300, USA*
[4]*UCD School of Physics, University College Dublin, Dublin 4, Ireland*

We examine the effects of long-range dipolar forces on metamagnetic transitions and generalize the theory of Condon domains to the case of an itinerant electron system undergoing a first-order metamagnetic transition. We demonstrate that, within a finite range of the applied field, dipolar interactions induce a spatial modulation of the magnetization in the form of stripes or bubbles. Our findings are consistent with recent observations in the bilayer ruthenate $Sr_3Ru_2O_7$.

Itinerant electron systems exhibiting metamagnetism, quantum criticality, and non-Fermi-liquid behavior continue to attract widespread experimental [1–3] and theoretical [4–6] interest, with the bilayer ruthenate $Sr_3Ru_2O_7$ as the most prominent example. Particularly surprising was the recent discovery of a new phase with increased resistivity as the quantum critical point is approached [2,3]. Different theories have been proposed for the nature of this new phase [6]. In this Letter, we show that dipolar magnetostatic forces in an itinerant metamagnet lead to domain formation in a small yet finite region of the temperature field phase diagram. These domains differ in the magnitude rather than the direction of the magnetization. Magnetic domain formation of this type was first proposed by Condon to explain de Haas–van Alphen measurements in Be [7]. Much later, Condon domains, which are formed and destroyed in each de Haas–van Alphen cycle, were observed directly using muon-spin-rotation (μSR) spectroscopy [8], and, recently, the domain pattern was observed in Ag by microscopic Hall probes [9]. The theory has been further refined in the context of the de Haas–van Alphen effect [10], but, to our knowledge, magnetic domain formation has not yet been considered in the context of metamagnetism.

We first consider briefly the standard phenomenological theory of itinerant metamagnetism starting from the free energy per unit volume $f(M, T)$ as a function of magnetization (produced by spin polarization of a metallic electron band) and temperature. The thermodynamic equation of state is $\mu_0 H^{\text{in}} = \partial_M f$, where μ_0 is the vacuum permeability and H^{in} is the magnetic field inside the sample. The differential susceptibility is $\chi = dM/dH^{\text{in}}$ or, equivalently, $\mu_0 \chi^{-1} = \partial_M^2 f$. By definition, metamagnetism occurs if the susceptibility has a maximum at a finite field, i.e., if $\partial_M^2 f$ has a minimum at $M = M_0$. In cases where $\partial_M^2 f$ becomes negative, a thermodynamic instability is produced where the magnetization jumps abruptly between two values M_1 and M_2 at which $H^{\text{in}} = H_m$ [Fig. 1(a)], determined by a Maxwell construction: $H_m = \partial_M f|_{M_1} = \partial_M f|_{M_2} = [f(M_2) - f(M_1)]/(M_2 - M_1)$. The location of the jump defines a line of first-order transitions in the H-T plane, which ends at a critical end point [Fig. 1(b)]. A quantum critical end point occurs if T_c is suppressed to zero as a function of additional parameters.

This standard picture must be supplemented to include magnetic dipolar interactions. We demonstrate this by translating an old argument by Condon [7] into the context of metamagnetism. The internal magnetic field is a combination of the external applied field H^{ex} and the field created by the magnetized sample $H^{\text{in}} \approx H^{\text{ex}} - nM$, where n is the demagnetization factor depending on sample shape and field orientation ($n = 0$ for a needlelike sample oriented parallel to the field and $n = 1$ for a thin film oriented perpendicular to the field). Thermodynamic stability is lost if H^{in} reaches H_m: From the low (high) field side, this occurs when $H^{\text{ex}} = H_{c1} = H_m + nM_1$ ($H^{\text{ex}} = H_{c2} = H_m + nM_2$). Instead of a single first-order transition, there is a finite region $H_{c1} < H^{\text{ex}} < H_{c2}$ where the uniformly magnetized state is unstable [Fig. 1(b)]. In this region, as we will show, magnetization forms domains with $M = M_1$ or M_2.

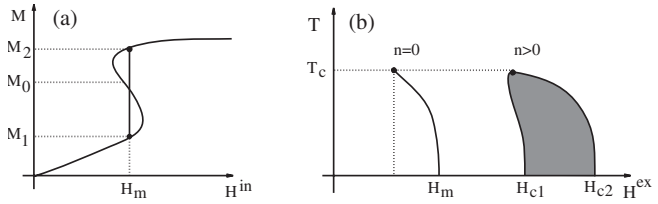

FIG. 1. (a) Magnetization as a function of the local internal magnetic field H^{in} with a jump at field H_m. (b) Schematic phase diagram in the H-T plane. For $n = 0$, there is a line of first-order transitions terminating at a critical end point. We assume that H_m is a decreasing function of temperature, reflecting the fact that entropy increases with increasing magnetization in itinerant metamagnets [5]. The gray area indicates the region of phase separation for $n > 0$.

A complete theory is based on the free energy functional for a spatially varying magnetization $M(\mathbf{r})$ parallel to the z axis [11]

$$F = \int d^3r[f(M) + K(\nabla M)^2] + E_d, \qquad (1)$$

where K is a parameter controlling the stiffness, and

$$E_d = \frac{\mu_0}{8\pi} \int d^3r \int d^3r' M(\mathbf{r})\Lambda(\mathbf{r}-\mathbf{r}')M(\mathbf{r}'), \qquad (2)$$

with $\Lambda(\mathbf{r}) = (r^2 - 3z^2)/r^5$ as the dipolar magnetostatic energy. The equilibrium magnetization profile $M(\mathbf{r})$, which minimizes $F - \mu_0 \int d^3r H^{\rm ex} M$, is determined by a competition between domain wall (DW) and dipolar energies. Below, we discuss its properties in the different regions of the phase diagram.

Close to the critical temperature, one may expand f in powers of $m(\mathbf{r}) = M(\mathbf{r}) - M_0$, where M_0 is the local minimum of $\partial_M^2 f$. Hence,

$$f(M) = f(M_0) + \mu_0 H_0 m + tm^2 + um^4 + O(m^5), \qquad (3)$$

where $\mu_0 H_0 = \partial_M f|_{M_0}$. All the parameters M_0, H_0, and t are temperature-dependent. Apart from the linear term which shifts the critical point to finite fields, we obtain the standard theory of an Ising ferromagnet with dipolar interactions [12]. There is no third-order term by construction, but other odd terms such as m^5 are permitted. For simplicity, we now consider an infinite film of thickness D. For this geometry with the field direction perpendicular to the slab, the demagnetization factor is $n = 1$. If the magnetization is independent of the z coordinate, the quadratic part of F in powers of m is $D \int d^2q\omega_q |m_{\mathbf{q}}|^2/(2\pi)^2$, where $m_{\mathbf{q}} = \int d^2r e^{i\mathbf{q}\cdot\mathbf{r}} m(\mathbf{r})$ and $\omega_q = t + Kq^2 + \mu_0(1 - e^{-qD})/(2qD)$. We assume that the sample is sufficiently thick that e^{-qD} may be neglected. No matter how small the dipolar interaction may be in relation to the spin stiffness, the instability always occurs at a finite wave vector $q_0 = (2l^2D)^{-1/3}$, where $l^2 = 2K/\mu_0$, giving sinusoidal modulations of the magnetization with wavelength $d = 2\pi/q_0$. On following the line $H^{\rm ex} = H_0 + M_0$ in the $H^{\rm ex}$-T phase diagram from high temperatures, there is a second-order transition from the uniform to the modulated phase as soon as the instability condition $t < -\frac{3}{2}\mu_0(\frac{l}{2D})^{2/3}$ is met. For values of the external field different from $H_0 + M_0$, both bubble- and stripe-modulated phases may be stabilized within mean-field theory, and the transitions are weakly first-order [12]. In each case, the modulated phase consists of a smooth, sinusoidal spin-density wave on top of the uniform magnetization background.

When $T \ll T_c$, the double-well structure of $g(M) = f(M) - \mu_0 H_m M$ becomes more pronounced, such that sinusoidal magnetization oscillations are no longer favored. The sample splits into domains of constant magnetization M_1 and M_2, separated by relatively sharp DWs. The determination of the domain structures then involves two independent problems. The first is the internal structure of the DW, which depends on the potential $g(M)$ and the stiffness K, and the second is the global domain pattern, which depends solely on the long-ranged dipolar interaction and the characteristic length $\xi = \sigma/(\mu_0 \Delta M^2)$, where $\Delta M = M_2 - M_1$ is the difference of magnetization of the two phases and σ is the DW energy per unit surface. The first problem is easily solved. The equilibrium magnetization profile of a single, flat DW satisfies $dM/dx = \sqrt{[g(M) - g(M_1)]/K}$, which leads to the following characteristic DW width and energy:

$$\lambda = \lim_{\epsilon\to 0} \frac{1}{\ln(1/\epsilon)} \int_{M_1+\epsilon\Delta M}^{M_2-\epsilon\Delta M} dM \frac{\sqrt{K}}{\sqrt{g(M) - g(M_1)}}, \qquad (4)$$

$$\sigma = 2\sqrt{K} \int_{M_1}^{M_2} dM \sqrt{g(M) - g(M_1)}. \qquad (5)$$

The second problem has been studied in great detail in the context of uniaxial (Ising) ferromagnets in the shape of thin platelets far below T_c [13,14]. In an intermediate range of the ratio D/ξ, the phase diagram as a function of magnetic field in the sharp-wall limit is very similar to that in the critical regime: a stripe phase in the center and a bubble phase at the border of the coexistence region separated by first-order transitions. The typical domain size is of order $d \sim (\xi D)^{1/2}$ and differs from the wavelength $2\pi/q_0$ in the critical regime. The domain structure is more complicated for thick samples ($\xi \ll D$), where an increasing number of wedge-shaped domains are formed close to the sample surface while the bulk domain size is typically $d \sim (\xi D^2)^{1/3}$ [14].

In order to interpolate between these two regimes, the critical regime close to T_c and the sharp-wall regime at low temperature, we propose the following ansatz, which depends on three variational parameters: λ, R, and d. For periodic stripe domains,

$$M_{\lambda,R,d}(x) = M_1 + \frac{\pi\lambda\Delta M}{d} \sum_{q_\nu} \frac{\sin(q_\nu R)\cos(q_\nu x)}{\sinh\frac{\pi q_\nu \lambda}{2}}, \qquad (6)$$

where $q_\nu = 2\pi\nu/d$. For a triangular lattice of cylindrical bubble domains,

$$M_{\lambda,R,d}(\mathbf{r}) = M_1 + \frac{2\pi^2\lambda R\Delta M}{\sqrt{3}d^2} \sum_{\mathbf{Q}_{\nu\mu}} \frac{J_1(Q_{\nu\mu}R)\cos(\mathbf{Q}_{\nu\mu}\cdot\mathbf{r})}{\sinh\frac{\pi Q_{\nu\mu}\lambda}{2}}, \qquad (7)$$

where J_1 is a Bessel function of the first kind and $\mathbf{Q}_{\nu\mu} = \frac{2\pi}{d}[\nu, \frac{(2\mu+\nu)}{\sqrt{3}}]$. In both cases, d is the period of the structure and μ, ν are integers. The interpretation of the parameters R and λ depends on the regime. If $\lambda \ll R, d$, the ansatz consists of domains of radius R with magnetization M_2 in a sea of M_1 and λ corresponds to the DW thickness. For $\lambda \gtrsim d$, the ansatz yields sinusoidal spin-density waves, because

higher Fourier modes are suppressed exponentially. The mean value around which the magnetization oscillates is controlled by R and the amplitude by λ. Examples of stripe and bubble configurations in both regimes are illustrated in Fig. 2.

After these general considerations, we now consider a model for a specific itinerant metamagnet, namely, a 2D electron system whose Fermi level is close to a logarithmic van Hove singularity (VHS). For this situation, the free energy $f(M,T)$ was calculated within the Hartree-Fock theory in Ref. [5]. Here we present an effective model which captures the primary physical features. At the Hartree-Fock level, $\mu_0\chi^{-1} = \partial_M^2 f \propto \rho_\uparrow^{-1} + \rho_\downarrow^{-1} - 2I$, where $\rho_\uparrow$ and $\rho_\downarrow$ are the thermally broadened densities of states at the Fermi level of up- and down-spin electrons, respectively, and I is the on-site Coulomb energy. At zero temperature, a singularity $\partial_M^2 f \sim 1/\ln|M - M_0|$ occurs, where M_0 is the magnetization at which one of the two electron species has its Fermi level exactly at the VHS. The main effect of a small, finite temperature is to provide a cutoff to this logarithm. These observations motivate the following effective free energy [Eq. (1)]:

$$\Delta f(M,T) = \{\delta - \gamma/\ln[(m/m_0)^2 + T/T_0]\}m^2, \qquad (8)$$

where m_0 and T_0 are positive parameters, $m = M - M_0$, and $\Delta f = f - f|_{M=M_0} - \mu_0 H_0 m$. Since Δf is an even function of m, it follows that $H_m = H_0$ for this model. The model of Eq. (8) is meaningful only for $m \ll m_0$ and $T \ll T_0$. The parameter γ is of the order vW/μ_B^2, where v is the volume of a unit cell and W^{-1} is the weight of the VHS. The parameter δ is proportional to the doping away from the quantum critical end point in the mean-field phase diagram neglecting E_d [5]. Dipolar interactions shift the quantum critical end point to $\delta_c = -\frac{3}{2}\mu_0(l/2D)^{2/3}$. For $\delta > \delta_c$, there is a metamagnetic crossover and for $\delta < \delta_c$ a first-order metamagnetic transition with a coexistence region below $T_c = T_0 \exp\{\gamma/(\delta - \delta_c)\}$. At zero temperature and assuming sharp DWs $\lambda \ll d$, we find using the Maxwell construction and Eqs. (4), (5), and (8):

$$\Delta M = 2m_0 \exp\{[\gamma + \sqrt{\gamma(\gamma - 4\delta)}]/(4\delta)\}, \qquad (9)$$

$$\lambda/l = [0.98 + O(\delta/\gamma)]\sqrt{\mu_0\gamma}/(-\delta), \qquad (10)$$

$$\xi/l = [0.42 + O(\delta/\gamma)](-\delta)/\sqrt{\mu_0\gamma}. \qquad (11)$$

The crossover between the critical and the sharp-wall regimes occurs at $1 - T/T_c \approx (2l/D)^{2/3}\mu_0\gamma/\delta^2$.

The entire $H^{\rm ex}$-T phase diagram for the model of Eq. (8) is shown in Fig. 2. It was obtained numerically by using the ansatz of Eqs. (6) and (7) and minimizing $F - \mu_0 \int d^3 r H^{\rm ex} M$. Figure 3 shows the mean magnetization as a function of $H^{\rm ex}$ at low temperature. The abrupt increase of the magnetization both on entry and on exit from the domain phase are clearly visible. Much smaller increases appear also at the transitions between bubble and stripe phases. The energy difference between the bubble and stripe solutions is extremely small, so that the precise domain structure will be susceptible to many details, e.g., lattice structure, impurities, and sample shape. The inset in Fig. 3 shows the temperature dependence of the magnetization for constant $H^{\rm ex}$. Note the increase of m with decreasing temperature in the uniform phase due to the diverging susceptibility at $H^{\rm in} = H_0$. Upon entering the domain phase, the magnetization increase is cut off, since the internal field $H^{\rm in}$ is locked to the nearly temperature-independent value of H_m. A small magnetization jump occurs at both first-order phase boundaries.

The existence of magnetic domains is known to increase the electrical resistivity due to DW scattering. In uniaxial ferromagnets, the DW resistivity shows a sharp increase upon entering the domain phase by tuning the magnetic field at a low temperature [15]. The resistivity in the direction perpendicular to oriented DWs is higher than in

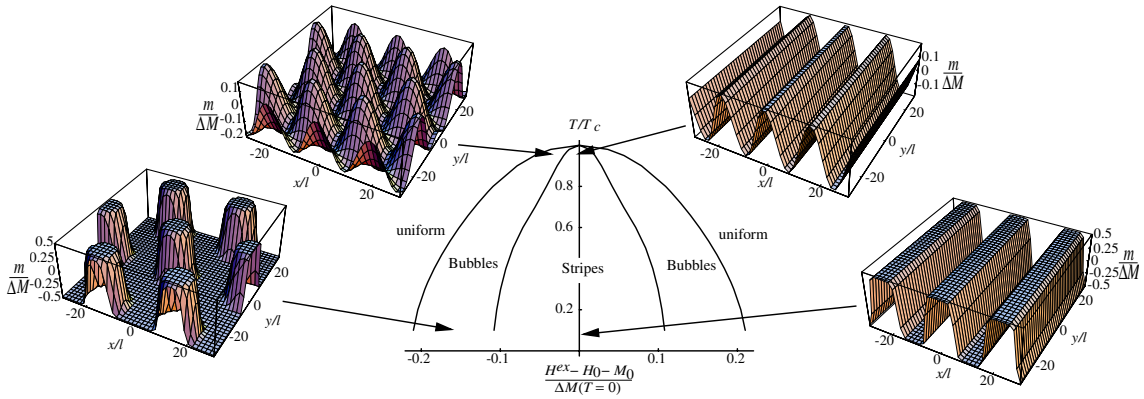

FIG. 2 (color online). Mean-field phase diagram as a function of external magnetic field $H^{\rm ex}$ and temperature T for the model of Eq. (8) within the ansatz of Eqs. (6) and (7). The parameters chosen were $\gamma = 100\mu_0$, $\delta = -8\mu_0$, and $D = 20l$, where $l = (2K/\mu_0)^{1/2}$. The insets show the magnetization profile $m(\mathbf{r}) = M(\mathbf{r}) - M_0$ at four different locations. The transitions are first-order at low temperature, weakly first-order in the critical regime $T \lesssim T_c$, and second-order at $T = T_c$.

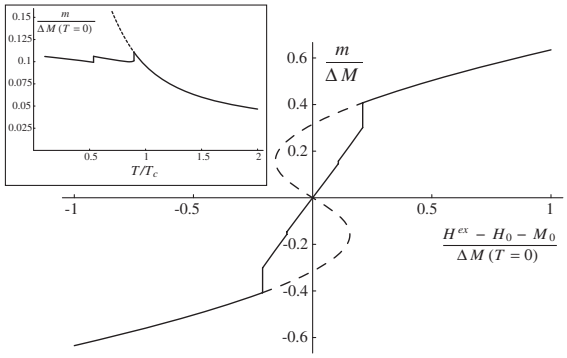

FIG. 3. Mean magnetization $m = M - M_0$ as a function of the external field at $T = 0.1T_c$. Model and parameters are as in Fig. 2. The dashed line indicates the (unstable) solution if the magnetization were uniform. The solid line was obtained with the ansatz of Eqs. (6) and (7). Inset: Temperature dependence of the magnetization along the line $H - H_0 - M_0 = 0.08\Delta M(T = 0)$.

the parallel direction [16] and even shows a nonmetallic behavior [17]. In contrast to ferromagnetic domains, Condon domains differ by the magnitude rather than the direction of their magnetization. This implies that properties such as the Fermi velocity vary across Condon DWs, leading to strong scattering of electrons, especially if the Fermi level is near a VHS, where electronic properties depend strongly on the band filling.

Our results are particularly relevant in view of the recent observation of a new phase in $Sr_3Ru_2O_7$ with a field oriented along the c direction [2,3]. The qualitative similarities between the phase diagram (Figs. 1 and 2) and the phase diagram of Ref. [3] are striking. Also, if metamagnetism is caused by a logarithmic VHS, then the domain phase is very sensitive to sample purity, because the VHS itself is very sensitive to impurities. The authors of Ref. [3] give a list of five key experimental facts which place rather tight constraints on any theory for the new phase. We note that all five points are compatible with magnetic domain formation. (i) DW scattering leads to an enhanced resistivity; (ii) the electrons are itinerant throughout the phase diagram; (iii) the mean magnetization increases both on entry and on exit from the domain phase as a function of field (cf. Fig. 3); (iv) a rise of the mean magnetization is cut off as the domain phase is entered from high temperature (cf. inset in Fig. 3); and (v) the domain phase exists only in a narrow range of applied fields. From the observed field range $\mu_0(H_{c2} - H_{c1}) \approx 0.2$ T [3] and the volume 78 Å^3 per Ru, we estimate $n\Delta M \approx 1.3\mu_B$/Ru. While this number appears rather large, it is not in error by orders of magnitude. Finally, we note that we have restricted ourselves to the simplest case of a field along the c axis. Other orientations require corrections beyond the scope of this letter. μSR, NMR spectroscopy, and microscopic Hall probe techniques could allow a direct detection of domain formation. For (quasi)static domains, the difference in local fields will lead to a characteristic splitting in the resonance lines as long as the corresponding dynamics is slow compared to the experimental time scales.

In conclusion, we predict that an itinerant electron system, in general, cannot undergo a first-order phase transition without breaking up into magnetic domains within a finite range of applied fields. While we cannot rule out other mechanisms explaining the unusual feature of the low temperature phase in $Sr_3Ru_2O_7$, our results show that a detailed experimental analysis is required to decide if mechanisms other than Condon domains underlie the unusual behavior.

B. B. thanks C. Capan, E. Demler, A. G. Green, Z. Q. Mao, B. Normand, C. Pfleiderer, A. Scholl, and A. Vishwanath for helpful and stimulating discussions. This work was supported by the NCCR MaNEP, the Swiss National Science Foundation, and the Science Foundation Ireland.

*Electronic address: binzb@berkeley.edu

[1] S. A. Grigera *et al.*, Science **294**, 329 (2001); R. S. Perry *et al.*, Phys. Rev. Lett. **86**, 2661 (2001); J. Hooper *et al.*, Phys. Rev. Lett. **92**, 257206 (2004); Z. Q. Mao *et al.*, Phys. Rev. Lett. **96**, 077205 (2006).
[2] R. S. Perry *et al.*, Phys. Rev. Lett. **92**, 166602 (2004).
[3] S. A. Grigera *et al.*, Science **306**, 1154 (2004).
[4] A. J. Millis *et al.*, Phys. Rev. Lett. **88**, 217204 (2002).
[5] B. Binz and M. Sigrist, Europhys. Lett. **65**, 816 (2004).
[6] A. G. Green *et al.*, Phys. Rev. Lett. **95**, 086402 (2005); H.-Y. Kee and Y. B. Kim, Phys. Rev. B **71**, 184402 (2005); C. Honerkamp, Phys. Rev. B **72**, 115103 (2005).
[7] J. H. Condon, Phys. Rev. **145**, 526 (1966).
[8] G. Solt *et al.*, Phys. Rev. Lett. **76**, 2575 (1996); Phys. Rev. B **59**, 6834 (1999); G. Solt and V. S. Egorov, Physica (Amsterdam) **318B**, 231 (2002).
[9] R. B. Kramer *et al.*, Phys. Rev. Lett. **95**, 267209 (2005).
[10] M. A. Itskovsky, G. F. Kventsel, and T. Maniv, Phys. Rev. B **50**, 6779 (1994); A. Gordon *et al.*, Phys. Rev. Lett. **81**, 2787 (1998); A. Gordon, I. D. Vagner, and P. Wyder, Adv. Phys. **52**, 385 (2003).
[11] Fluctuations $\mathbf{m}_\perp \perp \mathbf{H}^{\rm ex}$ are suppressed by a mass term $(\mu_0 H_0/2M_0)\mathbf{m}_\perp^2$, as is seen by expanding $f(|\mathbf{M}|)$ to second order in $\mathbf{m} = \mathbf{M} - \mathbf{M}_0$. For $Sr_3Ru_2O_7$ [1], we have $H_0/M_0 \approx 1.7 \times 10^2 \gg 1$, and, hence, the mass is much larger than the dipolar energy scale. This is in contrast to the isotropic ferromagnet; see, e.g., R. Arias and H. Suhl, Phys. Rev. B **51**, 979 (1995).
[12] T. Garel and S. Doniach, Phys. Rev. B **26**, 325 (1982).
[13] J. A. Cape and G. W. Lehmann, J. Appl. Phys. **42**, 5732 (1971).
[14] J. Kaczér, IEEE Trans. Magn. **6**, 442 (1970); A. Hubert, Phys. Status Solidi **24**, 669 (1967).
[15] D. Ravelosona *et al.*, Phys. Rev. B **59**, 4322 (1999).
[16] M. Viret *et al.*, Phys. Rev. Lett. **85**, 3962 (2000).
[17] M. Feigenson *et al.*, Phys. Rev. B **67**, 134436 (2003).